OPTIMIZATION OF HELIOSTAT FIELD LAYOUT FOR THE BEAM – DOWN OPTICS

by
Akiba Segal
Weizmann Institute of Science
Chemical Research Support Department
Solar Optics Design and Mathematical Modeling Unit

Report
SFERA, WP.13, Task 2, July 2011

Last revision 30 July 2011

1. INTRODUCTION

The experience gained during the last three decades in developing applications of concentrated solar energy shows that higher conversion efficiency of solar energy to electricity can be achieved only at high temperatures (more than 1100 K) (Segal and Epstein, 2000). At these temperatures, the radiation emitted from the receiver at the working temperature becomes the main mechanism of thermal losses depending on the size of the receiver aperture. It is obvious that, in order to increase the receiver efficiency, the solar energy must be introduced into the receiver at higher concentrations. To reach high concentrations at the receiver aperture it may not be sufficient to improve the performance parameters of the primary concentrator (the field of heliostats), but a secondary concentration is often required. As any optical device, the secondary concentrator has its own inherent losses, which reduce the total optical efficiency. Introducing the secondary concentrator has a substantial effect on the optimal shape, size and arrangement of the primary concentrator. The receiver coupled with its secondary concentrator, i.e., the **receiver concentrator** (**RC**), is a **Compound Parabolic Concentrator** (**CPC**) type (Winston *et al*, 2005). This optics has been first published by Segal and Epstein (1997). It becomes a combined unit, where both the thermal and the additional optical losses have to be analyzed and considered (Segal and Epstein, 1999a).

Other important losses in a thermal system are those associated with the heat transport from the solar receiver to the energy converter (e.g., a gas turbine). In order to minimize these losses, the turbine is installed close to the receiver. In usual large solar power plants, the receiver and the turbine together with auxiliary equipment are heavy burden to be supported on the top of a tower structure. An alternative option is to invert the path of the solar rays originating from a heliostat field in a way that the solar receiver and the above equipment can be placed on the ground. In order to carry out this optical path inversion, a supplementary reflector has to be installed. This causes the rays oriented to the aim point of the field to be reflected down to the RC entrance located near the ground. From an optical point of view, only a reflective surface having two foci is capable of this mission, namely, each ray that is oriented to one of its foci (which coincides with the aim point of the heliostat field) will be reflected to the second focus positioned at the entrance plane of the RC. From mathematical point of view, this surface is a quadric, namely, a hyperboloid (with two sheets, of which only the upper one is used), or an ellipsoid. A hyperboloidal mirror placed at a certain distance below the aim point of the heliostats, can achieve this goal. Similarly, an ellipsoidal mirror placed at certain height above the aim point can

provide comparable results. The performances of these two types of reflectors have been compared by Segal and Epstein (2001). The comparison shows that the hyperboloidal surface is definitely more effective than the ellipsoidal one, so that we will consider further only a hyperboloid mirror. This optical system based on this hyperbolic mirror as reflector of the rays back to the ground is named **Tower Reflector (TR)**, also using the name **Beam-Down (BD)** for the entire optical system.

The present work describes our experience accumulated along two decades in optimization of a heliostat field used for the classical tower optics (Section 3) as starting point for the description of the methodology used for optimization of heliostat field in the frame of BD optics (Sections 4-6).

2. MATHEMATICAL BACKGROUND

A ray of light can be described mathematically as a straight line as follows:

$$x = x_i + k \cdot u_x; \quad y = y_i + k \cdot u_y; \quad z = z_i + k \cdot u_z \tag{1}$$

where: (x_i, y_i ,z_i) are the coordinates of the origin of the ray (on the surface of the heliostat) and (u_x, u_y, u_z) are the components of the ray's unit vector of direction. This ray is intersected with the reflective surface (hyperboloid) having the following general equation:

$$f(x,y,z) = \frac{(y_p t + z_p)^2}{a^2} - \frac{x_p^2(1+t^2) + (y_p - z_p t)^2}{b^2} - t^2 - 1 = 0; \quad t = \frac{y_o - y_c}{z_o - z_c} \tag{2}$$

where: $x_p=x–x_o$, $y_p=y–y_o$, $z_p=z–z_o$, subscript *o* represents the quadric center and subscript *c* represents the center of the secondary concentrator entrance, in the tower system coordinates (x,y,z), ***a*** and ***b*** being the hyperboloid semi axes. The surface described by Eq. (2) has been written in a general way, including the option to tilt the axis of the quadric surface in the yOz plane (this is the north-south plane because the axis Oy is supposed to be oriented to the north) (see Section 3). The coordinates of the point of intersection between the ray and the reflector surface, (x_s,y_s,z_s), are obtained by solving the system of Eqs.(1) and (2) for the parameter *k*. The normal at the point of the intersection to the particular surface is calculated by solving the following partial derivatives:

$$n_x = \frac{\partial f / \partial x}{\|n\|}; \quad n_y = \frac{\partial f / \partial y}{\|n\|}; \quad n_z = \frac{\partial f / \partial z}{\|n\|}; \quad \|n\| = \left[\left(\frac{\partial f}{\partial x}\right)^2 + \left(\frac{\partial f}{\partial y}\right)^2 + \left(\frac{\partial f}{\partial z}\right)^2 \right]^{1/2} \tag{3}$$

Finally, the reflected ray has the direction u^r with the components:

$$u_x^r = u_x - 2\,sc \cdot n_x; \quad u_y^r = u_y - 2\,sc \cdot n_y; \quad u_z^r = u_z - 2\,sc \cdot n_z;$$
$$sc = n_x u_x + n_y u_y + n_z u_z \tag{4}$$

The intersection between the reflected ray and the entrance plane of the RC is calculated by substituting in the system of Eq. (1) the coordinates (x_s,y_s,z_s) of the intersection point on the reflector surface, the direction of reflected rays u^r and solving for k the equation $z_c=z_s+ku_z^r$, z_c being the z coordinate of the RC entrance. The coordinates x_c and y_c in the entrance plane to the RC are consequently calculated by Eq. (1).

Numerical results of the calculations and assumptions used as a basis for them are depicted later for various practical cases.

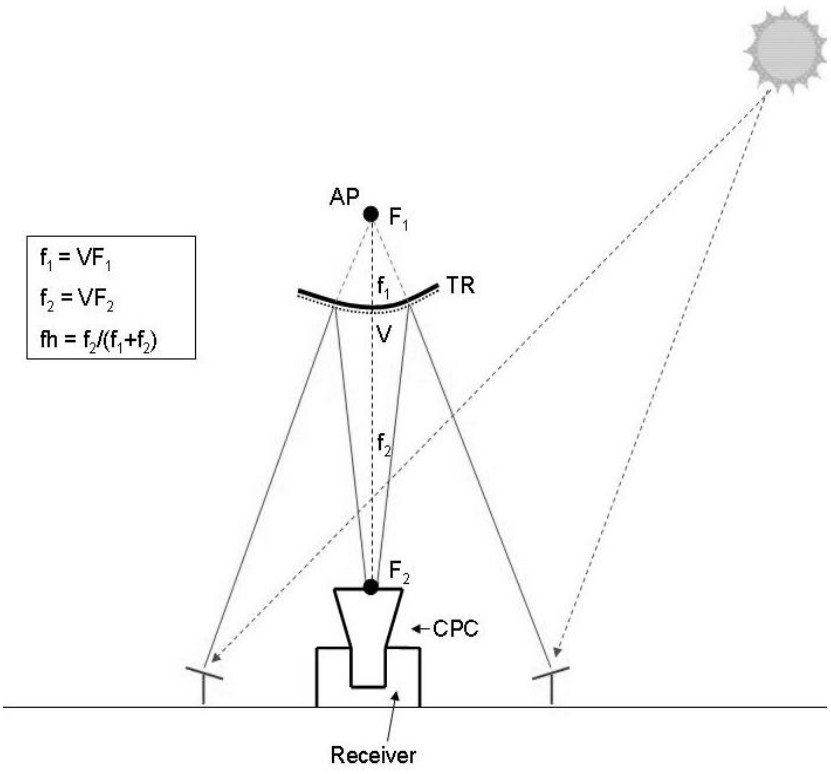

Fig. 1 Beam Down optics

3. THE PRINCIPLES OF A TOWER REFLECTOR

A tower reflector is an optical system comprised of a hyperboloidal mirror (with two sheets; the focal line is vertical; only the upper sheet is considered in this optical system) where the upper focal point coincides with the aim point of a heliostat field and its lower focal point is located at a specified height,

coinciding with the entrance plane of the RC on the ground level (Fig. 1). This system was proposed by Rabl (1976) and further investigated by Winter *et al.* (1991), and, at the Weizmann Institute of Science, by Epstein and Segal (1998), Kribus *et al.* (1997, 1998), Yogev *et al.* (1998), Segal and Epstein (1997, 1999a,b, 2000, 2001). The beams from the heliostats are reflected downward by this mirror. The optics of a tower reflector requires the use of the RC if high concentrations are desired, because the quadric surface mirror always magnifies the sun image. The magnification is defined here as the ratio between the image diameter at the second focal plane and the image diameter at the aim point of the heliostat field. This magnification is a function of the ratio of the distances between the mirror vertex to the upper and to the lower foci (Fig. 2 – ***M*** vs. f_2/f_1). Evidently, this function is linear in a large range of the ratio f_2/f_1. In a two-dimensional model, the linearity is absolute for the entire range but, in a real three-dimensional model, the linearity is perturbed by the image distortions caused by the aberrations occurring at a smaller f_2/f_1 ratio. The magnification depends also on the ratio between the radius of the field and the height of the aim point. It decreases as the radius of the field increases for the same height of the aim point (Fig. 3), although for a larger field, the image diameter at the aim point is larger due to the larger distance to the last row of heliostats.

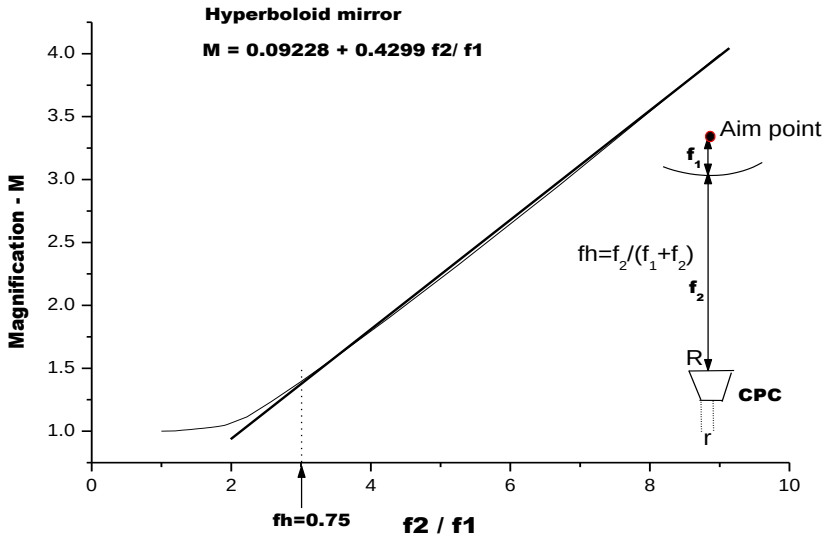

Fig. 2 Image magnification in lower focus function of ratio f_2/f_1

Moving the hyperboloidal mirror down, towards the lower focal point causes the size of the image to be smaller. However, this displacement results in two undesirable effects (Fig. 4). In the case of hyperboloidal mirror, the size of the reflector increases as its height above the heliostats is decreased. The acceptance angle of the rays arriving to the ground RC is also increased. The acceptance angle determines the ability of the RC to concentrate the radiation arriving at its entrance (Welford and Winston, 1989).. One can define $\boldsymbol{fh = f_2/(f_2+f_1)}$ as the fractional position of the vertex of the hyperboloid from the height of the aim point (assuming that the lower focus of the hyperboloid is at the heliostat level), obviously ½ <***fh***<1.

It will be shown that the optimal position of the tower reflector (defined as location that produces the maximum concentration at the receiver entrance) is found between ***fh***=0.75 and ***fh***=0.85.

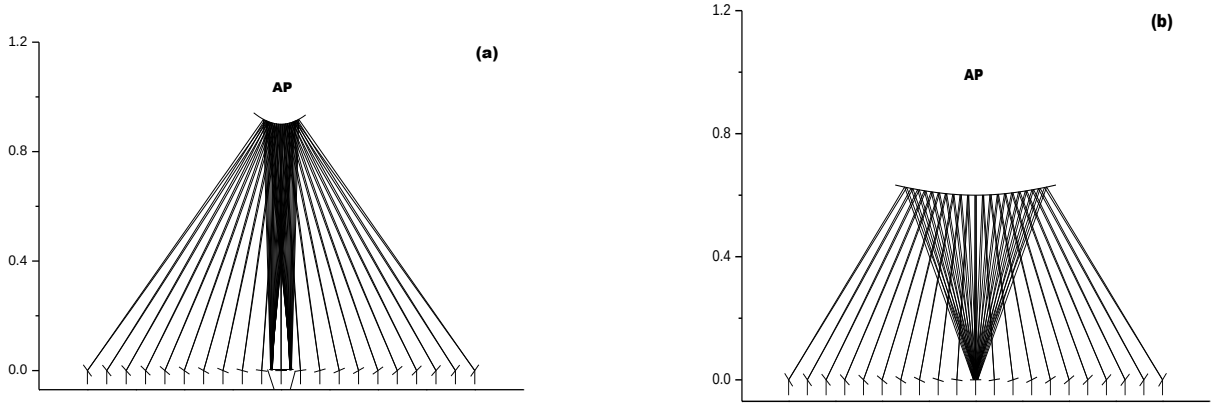

Fig. 3 Optical behavior of hyperboloid mirror

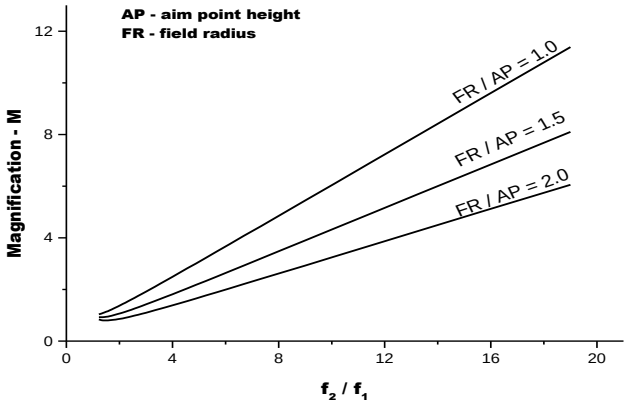

Fig. 4 Magnification of image vs. ratio f_2/f_1 for different field radii

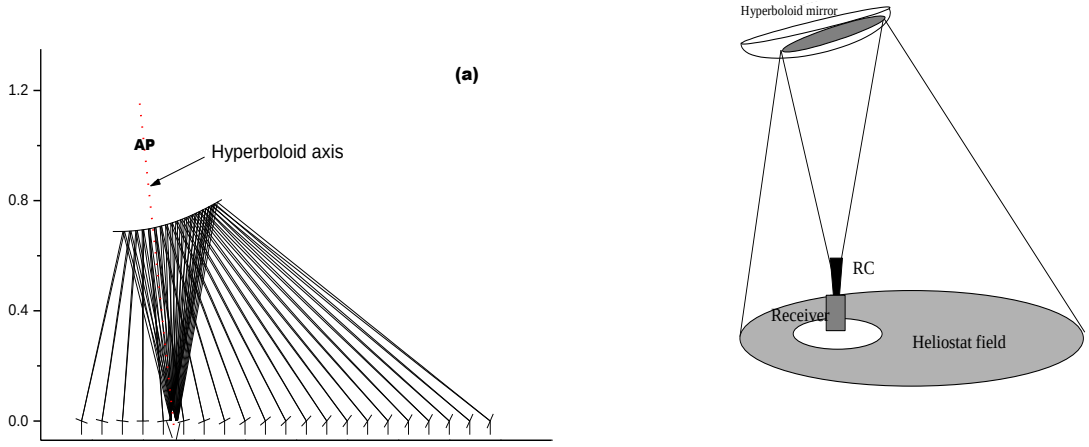

Fig. 5 Upper mirror axis is tilted when the field is asymmetric

In the Northern Hemisphere, at a typical latitude range of 25–35°, the heliostats are arranged in a northern field or, in the case of a large surrounding field, the northern part is usually larger than the southern part. In these cases the quadric axis must be tilted if a vertical position of the RC is requested (Fig. 5). For a hyperboloidal mirror, this tilt is made by moving slightly the lower focus in the northern direction relative to the aim point.

An optimum position exists for a reflector that maximizes the receiver efficiency. As illustrated in Fig. 8, the optimum situation occurs when the edge rays from the heliostat field, after reflection from the tower mirror, coincide exactly with the edge rays of the RC. Mathematically, a new concept can be introduced: transformation by reflection from a quadric surface. The optimum is achieved when the volume in phase space (Winston *et.al*, 2005) of the rays leaving the heliostats is equal to the volume in phase space of the reflected rays arrived to the RC. Fig. 6a shows the acceptance angle, the entrance radius of the RC and its exit radius, as a function of the reflector position, ***fh***, for the specific example of the small field (Segal and Epstein, 1999a). The maximum average concentration level at the receiver aperture is obtained when the ratio ***fh*** [$=f_2/(f_1+f_2)$] between the distance from the apex of the mirror to the lower focus and the distance between the two foci is equal (in this particular case) to 0.73. Nevertheless, as shown below, the highest concentration is only an indication of the maximum efficiency. This position does not provide automatically the optimum for the receiver efficiency. Only a

detailed calculation for optimization, as presented by Segal and Epstein (2000), will result in a position that assures the highest receiver efficiency.

Fig. 9b shows the situation where two different aim points for the heliostat field are considered. For the higher aim point, the RC's acceptance angle is smaller for the same relative position ***fh*** (equivalent to the same ratio f_2/f_1) of the hyperboloidal mirror. As already discussed, the same f_2/f_1 implies the same magnification, but, because the virtual image at the aim point is larger for the higher aim point, the image at the entrance of RC will be larger in the case of higher aim point (Fig. 6b), and, as a result of combination of the radius of this image and the corresponding acceptance angle, the exit radius from RC will have approximately the same dimension. Therefore, the height of the aim point has almost no optical influence on the possible concentration observed in these cases. In this analysis we considered only the optics of the tower reflector and the RC (as an ideal device). Moreover, a higher aim point has the general advantage of lower blocking and shadowing in the field of heliostats; as a result, more energy will arrive to the receiver when using a higher aim point. In any case, in order to find the optimal position of the reflector, its height is varied according to a certain strategy. For each position, the optimal geometry of the RC is established following the method described by Segal and Epstein (1999b). A particular case is worth mentioning. This is when the mirror is positioned at exactly equal distance between the aim point and the entrance plane of the RC (***fh*** = 1/2). In this case, the hyperboloid becomes a flat mirror, the magnification is 1 and the aim point image is exactly reflected to the RC entrance plane. This option is not practical because the radius of the mirror will be half of the heliostat field radius, and therefore, this choice is disregarded.

The energy flux distribution of the sun image at the entrance plane of the RC (the lower focal plane) has a peak at the center (Fig. 7). As one moves radially from the center to the edges of the image, the flux decreases. Attempting to capture the entire image into a single RC will results in diluting the average flux at its entrance. This is disadvantageous from a thermodynamic point of view. Since the reflective tower magnifies the sun image at the RC entrance plane, a single concentrator capable of collecting most of the energy will have a large opening and the losses by reradiation will be high. Therefore, the optimization method, as described in the next section, is aimed at reducing the size of the RC opening, accepting some increasing of the spillage losses. A possible solution was proposed by Ries *et al.* (1995) for exploiting the edge part of the image for lower temperature applications or for

preheating purposes, while the central portion of the image can be used for the topping of the thermodynamic cycle. This approach can increase the total efficiency of a power conversion system.

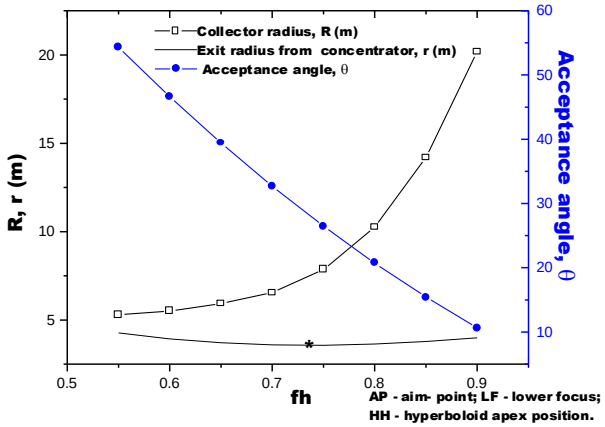

Fig. 6

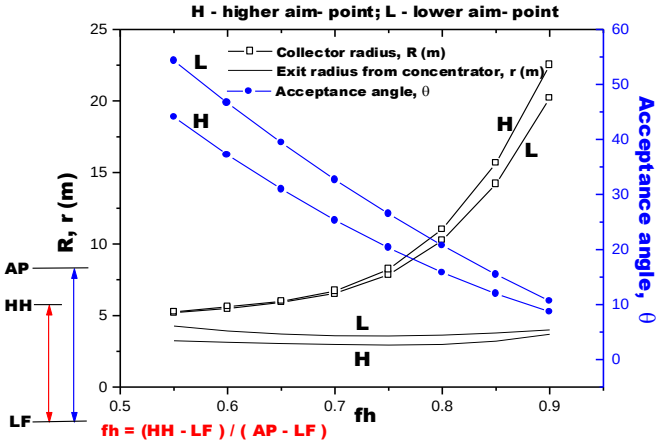

Fig. 7

Fig. 8 illustrates the flux distribution at the RC entrance plane and the power that can be absorbed by the receiver as a function of the distance from the center, for the two positions of the TR, as depicted in Fig. 4a and 4b (*fh*=0.9 and *fh*=0.6, respectively). As expected, when the reflector is in a lower position, the flux decreases sharply with the distance from the center of the image. As a result, the radii of the central collector and preheaters are relatively small, compared with the situation where the hyperboloid is in a higher position. But this is not the only parameter that determines the hyperboloid position. A large reflector area means a lower average (and peak) flux on the reflector itself. In addition, the partition between the size of the central RC and the peripheral preheaters, as well as their acceptance angles, are subject to an optimization search aimed at maximizing the efficiency of the entire system (Segal and Epstein, 1999a, b, 2000).

The criterion for this optimization can be the maximization of the receiver thermal efficiency (defined as the ratio between the net power delivered to the thermal process and the total power arriving at the RC's entrance plane) (Segal and Epstein, 1999a), or, if economic parameters are introduced, the minimization of the cost of kilowatt thermal power absorbed by the receiver. In either case, the concentration at the receiver entrance is only an indicating parameter for better efficiency but not the ultimate criterion for optimization.

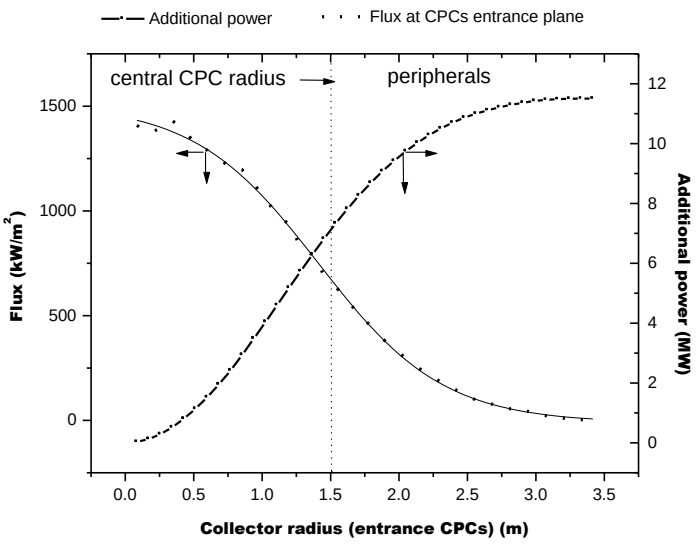

Fig. 8 Flux and power collected vs. collector radius

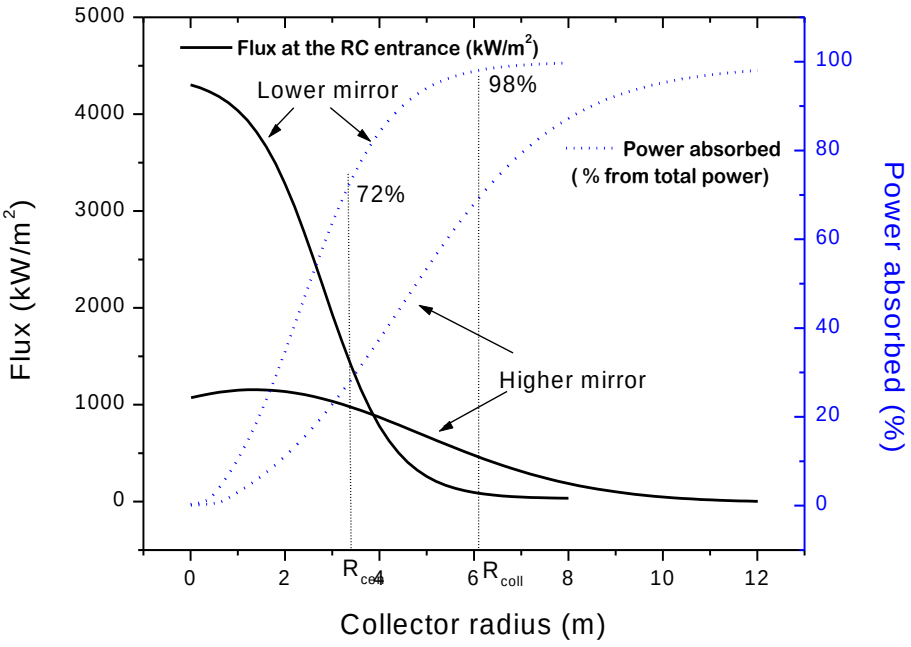

Fig. 9 Dependence of flux and power collector to aim-point height

4. THE METHODOLOGY FOR HELIOSTAT FIELD OPTIMIZATION BASED ON BEAM DOWN OPTICS

4.1 The optimum boundary for a surrounding field

The BD optics has been successfully used recently for testing in different projects at the Weizman Institute of Science. There is currently sufficient data on this technology to evaluate its up-scaling for commercial uses.

The sizing of a TR is directly linked to the layout of the heliostat field and the geometry of the ground secondary concentrator (CPC). It depends on its position relative to the aim point of the field, amount of spillage around it and the allowable solar flux striking the TR. Its position influences the size of the image at the entrance plane of the ground CPC and the spillage around the CPC aperture. The spillage around the CPC is also directly related to the exit diameter of the CPC (equal to the entrance opening of the solar reactor, matching the CPC exit) and therefore linked to the input energy concentration, thermal losses and working temperature in the reactor. Restrictions on the size of the exit of the CPC can influence the entire design of the optical system. But an optimized heliostat field is an essential part of BD optical system and we have enough experience to build such field. The methodology for construction of the corresponding field layout will be exposed in this Section.

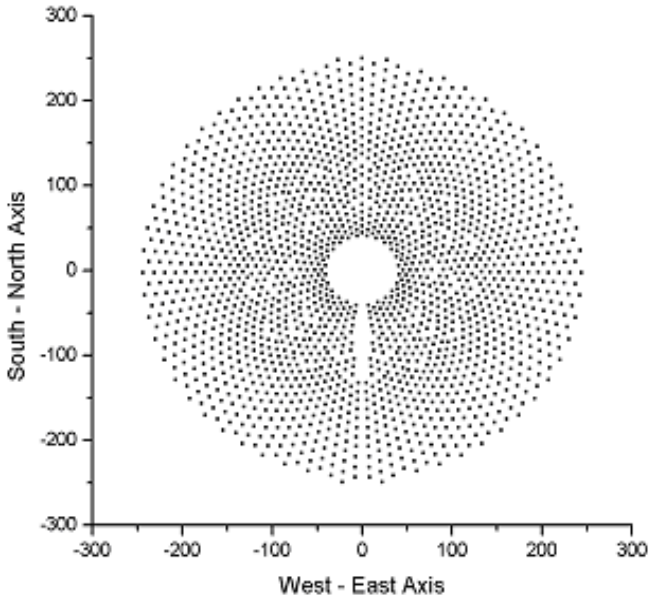

Fig. 10 Symmetrical circular surrounding field (non-optimized)

A symmetrical circular surrounding field (Fig.10) is not optimized since the southern heliostats are less effective (in the Northern Hemisphere) than the northern heliostats and therefore a real surrounding field will be shifted from the center to north and stretched in the north-south axis to form an elliptical shape. But this layout can be seen as the first iteration for finding the best corresponding field. A number of methods for optimization of the large fields have been proposed in the past (Lipps and Van't Hull, 1978) A recent attempt is by Sanchez and Romero (2006), where the arrangement of the heliostats is starting with the first row and supplementary rows are added so that the normalized annual energy is maximized. In this method the rapprochement of heliostats below the mechanical limits is refrained by introducing a void ring between two consecutive rows of heliostats (see also WinDelsol (2002)).
The optimal design of a collector heliostat field involves determining the optimal location of each heliostat in the field and the boundary contour of this field so that the daily, monthly or annually performances of the entire field will optimally meet the requirements.

In general, the figure of merit used for this optimization is the ratio of the total system cost to the total energy delivered by the whole system. In this case, the optimization will consists in finding the minimum for this figure of merit. Referring to the optimization of the collector field subsystem, the previous figure of merit is equivalent to the maximization of another figure of merit which is the average energy delivered by a single heliostat from the field. (This approach ignores in the first approximation the cost of the land and the wiring). In order to calculate this average energy per heliostat, the coordinates of each heliostat in the field must be determined. At the same time, this optimization cannot be independent of the optimization of the balance of the central solar plant, especially the height of the tower/aim- point. This is important data input for the optimization of the collector subsystem. Therefore, we will express all the lengths in the field in units of tower/aim-point height (in other words the tower height is equal to *one unit* length **UL**)

The azimuthal distance and radial separations can be determined by various empirical correlations given by Kistler (1986) or Winter et al. (1991) These correlations, although mathematically are not likewise, give very closed results. For a given field (i.e. the exterior boundary is fixed at $r_{\max}$) we found that both these correlations leads to remarkable linearity (more than 98%, as can be seen in Fig. 11a) between the radial separation and the distance to the tower:

$$\Delta r = (u \cdot r + v) \cdot h_t \qquad (5)$$

where u and v are functions of r_{max} and h_l is the typical heliostat dimension. A graphical dependence of these functions vs. r_{max} is shown in the Fig. 11b.

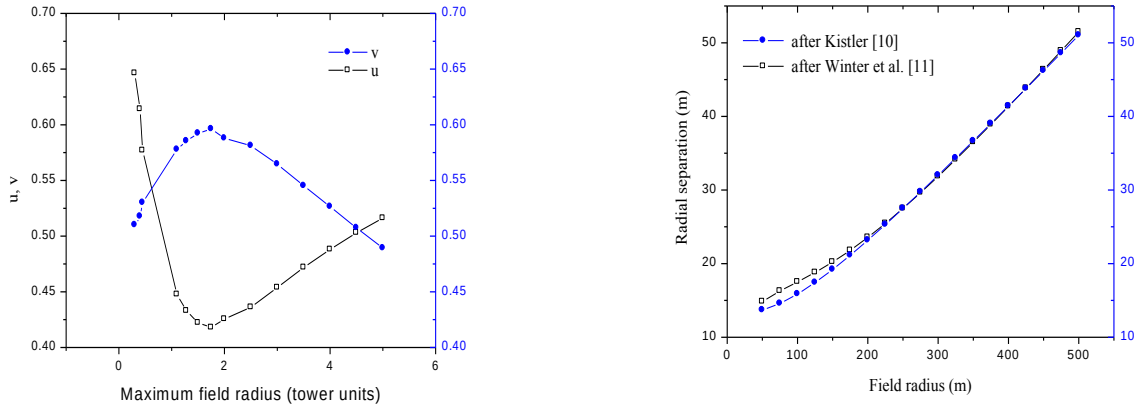

(a) **(b)**

Fig. 11 Linear coefficients from eq.(5) vs. field radius

The criterion of optimization is the maximization of the annual solar contribution of an average heliostat into a virtual receiver aperture. This aperture is circular, placed in horizontal plane and centered relative to the field's aim-point. Considering a field with exterior boundary having three parameters*: u*, *v* and *w* (*w* being the azimuth separation between two neighboring heliostats in the farthest row) and based on the radial linear separation given by (Eq. 5) and radial staggered layout with slip planes [13], the entire field is completely and precisely defined from the farthest row inwards, to the closest row to the tower reflector. Free space around the tower is allocated not only for optical reasons, but also for technical requirements.

The method proposed by Segal and Epstein (1996), Segal(1999),maximizes the ratio E_t / N_h, where E_t is the total annual energy delivered to the target and N_h the number of heliostats in the field. Initially, the field is assumed circular and sized to deliver power larger than the nominal specified power at the design point. This requires an optimization in three dimensions (*u*, *v*, *w*) which can be solved assuming the field is built based on the above described algorithm. The result is an optimal field configuration with maximum average contribution of each heliostat integrated over the year and having the power at design point larger than the required nominal power. Fig. 12 presents the isoenergetic curves of annual contribution of each heliostat in the whole field relative to the most efficient heliostats designated with efficiency equal to 1. Array of the less efficient heliostats in the field is established in the inverse order

of their contribution and, finally, the heliostats with the lowest annual energetic contribution are eliminated until the desired power is achieved at the design point. The remaining heliostats configure the optimal field. In the last step a slight compromise is made to shape the field in compliance with the most appropriate elliptical boundary. This boundary has its center shifted by a certain distance to North relative to the tower reflector [15].

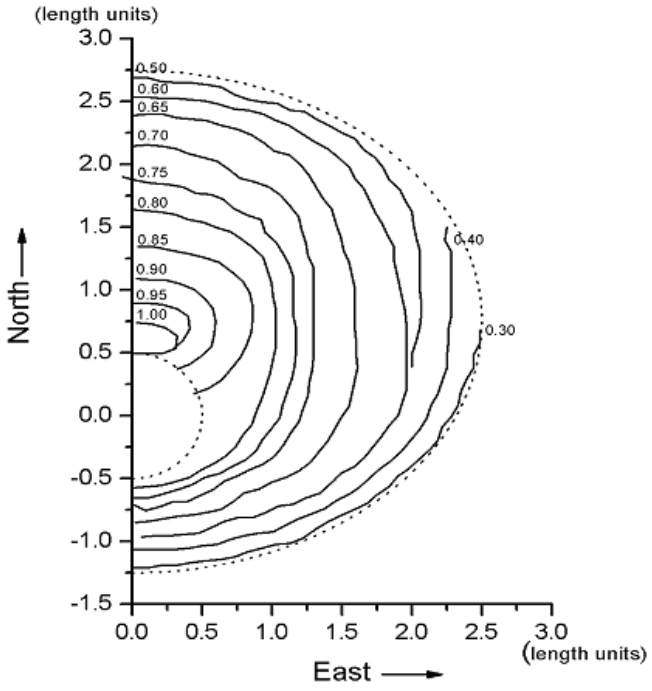

Fig. 12 Isoenergetic curves of annual contribution of heliostats

4.2 Dimension of tower reflector and ground concentrator

As described in the previous section, the field boundary is fixed after the optimization process to match the nominal power requirement. Adopting the definitions outlined in Section 3, the sizing of the tower reflector and the ground CPC can be best illustrated through the following specific example. A field having an elliptical boundary is assumed, having semi-axes of $v = 2.8*UL$ on South-North axis and $w = 2.2*UL$ on the East-West axis. Also the center of the ellipse boundary is shifted by $e = 0.8UL$ north to the vertical line drawn from the aim-point (see fig.13 where UL=100m). In addition, as described by Segal and Epstein [15], in such a field, the tower reflector axis must be tilted so that the hyperboloid

lower focus is moved north relative to the vertical from the aim-point (upper focus) in order to preserve the verticality of the CPC cluster.

The equation of a hyperboloid having the Oz axis tilted with the angle τ with the vertical can be written as:

$$\frac{(y\cdot t - z - \xi)^2}{a^2} - \frac{\theta^2 x^2 + (y + z\cdot t - \eta)^2}{b^2} - \theta^2 = 0 \qquad (6)$$

where: $t = \tan\tau$; $\theta^2 = 1 + t^2$; $\xi = (t^2-\theta)/2$; $\eta = (1+\theta)\,t/2$; a, b being the hyperboloid semi-axes defined as in Section 2

Similar to the procedure developed in Section 2, a generic point ***P*** is determined on the field boundary having the coordinates (x_o,y_o,z_o), where $y_0 = e \pm \frac{w}{v}(v^2 - x_0^2)^{1/2}$ and $z_{o=}$ -d. A straight line PA, connecting ***P*** and the aim point ***A***, intersects the upper sheet of the hyperboloid (Eq. 6). The intersection of a reflected ray from this point on the hyperboloid with the lower focal plane is calculated. The image of the field boundary on this plane will be also an ellipse centered at $y = t = \tan\tau$. When varying the tilt angle τ, namely moving the position of lower focus to North, it can be observed that the elliptical image becomes close to a circle and the incidence angle of the rays originated from the various points ***P*** on the field boundary and reflected by the TR approaches the same value. In this point, the position of the CPC cluster will be vertical as desirable.

The reflective area of the entire heliostats field can be calculated by:

$$A_{ref} = \pi(v\cdot w - r_v^2)\cdot\delta \qquad (7)$$

The TR area as a fraction of the heliostat reflective area (S/A_{ref}) can be easily calculated now.

In order to evaluate the dimension of the sun's image at the ground CPC entrance plane after being reflected by the heliostat field and by the TR, one should consider the sun disk with its semi-angle Δ_s. The calculations are done for a bundle of rays originated from each point on the boundary of the field. The results of the image radius at the CPC entrance plane which includes e.g. 95% of the arriving rays and a corresponding acceptance angle are presented in Table 2.

This CPC can collect and transmit at least 95% of the power reaching its entrance plane. In the example indicated above (when ***f*** = *0.8*), the entrance radius of the CPC will be 0.0482 units and the acceptance angle 24°, which correspond to an exit radius of 0.0196 units. As previously discussed [8], for large

fields the exit aperture of a single CPC could be too big for specific application, and therefore a practical solution can be the use of a cluster of seven identical CPC units: one central and six peripherals that will intercept at least 95% of the full image at the CPC entrance plane. In the case of seven CPC units, each of them has the entrance radius 0.0187*UL*, exit radius 0.0073*UL* and height of 0.0614*UL*. The total reflective surface area of this cluster will be $S_{CPC} = 0.072\ UL^2$. This area is calculated as a fraction of the field reflective area ($S_{CPC} / A_{ref} = 1.4\%$). Shown in Table 1 is this fraction, calculated for different values of $\boldsymbol{f}$ ($0.5 < \boldsymbol{f} < 1$).

Table 1

fh	**Tilted** angle **(^{0})**	**r_i** **(UL)**	**z_i** **(UL)**	**r_s** **(UL)**	**z_s** **(UL)**	**S** **(UL^2)**	**S/A_{ref}** **(%)**	**acc** **(°)**	**CPC_r** **(UL)**	**CPC_{ex}** **(UL)**	**h_{CPC}** **(UL)**	**A_{CPC}** **(UL^2)**	**A_{CPC}/A_{ref}** **(%)**
0.65	9.6	0.1792	0.6602	0.5622	0.7319	0.910	17.2	49.0	0.0266	0.0201	0.0406	0.012	0.2
0.70	7.5	0.1527	0.7108	0.4693	0.7863	0.639	12.1	39.5	0.0309	0.0197	0.0613	0.020	0.4
0.75	6.4	0.1259	0.7604	0.3699	0.8288	0.397	7.5	31.0	0.0396	0.0204	0.0998	0.038	0.7
0.80	5.2	0.0922	0.8079	0.2888	0.8700	0.249	4.7	24.0	0.0482	0.0196	0.1523	0.066	1.2
0.85	3.9	0.0511	0.8536	0.2034	0.9028	0.130	2.4	17.5	0.0652	0.0196	0.2690	0.145	2.7
0.90	2.7	0.0126	0.9004	0.1431	0.9432	0.069	1.3	12.0	0.0918	0.0191	0.5217	0.367	6.9

Table 1. Optimized field: comparison between the results obtained by calculation for a real field of heliostats r_i / r_s – inferior / superior radius that delimits on the TR the illuminated surface; z_i / z_s – corresponding heights of the illuminated surface limits; acc – acceptance angle; CPCr – CPC entrance radius; CPCex – CPC exit radius; h_{CPC} – CPC height; A_{CPC} – total CPCs area

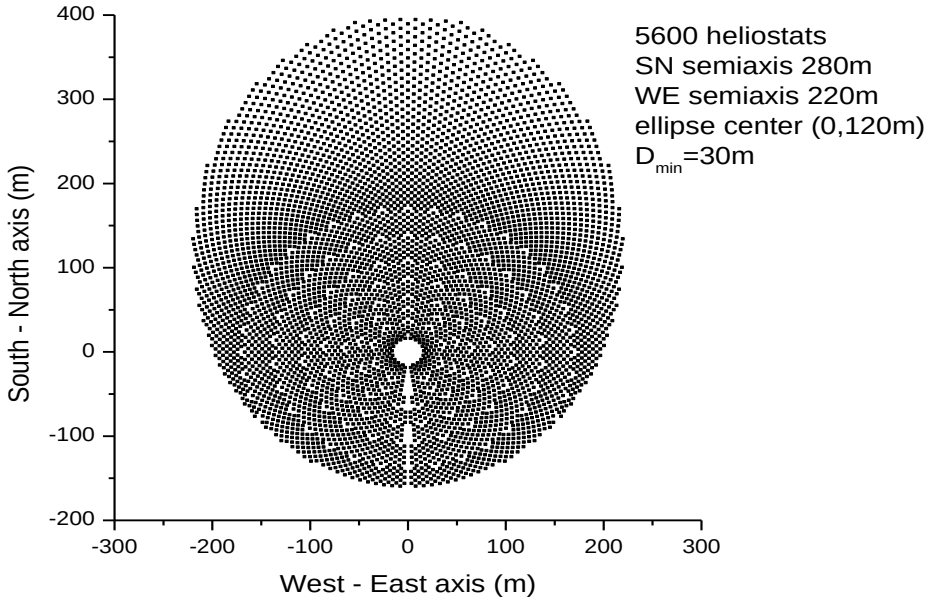

Fig. 13 Optimized heliostat field used as first guess in Sect.4.3

4.3 Optimization of a real heliostat field based on beam-down optics.

The field presented in Fig.13 is optimized following the method proposed by Segal and Epstein ( ), therefore it has the best row separation, also the azimuthal angles, as a result the shadowing and blocking will be reduced at minimum possible (at least at the Design Point), but it constitutes only the starting point for a concrete requirements.

Let's exercise the method of layout optimization on a concrete example:

We will consider UL=100m. The target is a circle having area equivalent with the entrance area of 1+6 CPCs having yet unspecified dimensions. The restriction is that each CPC will be connected with a receiver / preheater (identically) having total area equivalent with the area of in a circle of diameter 0.1UL. The exit angle from CPC will be maximum 75^o. A first guess gives for exit diameter from CPC to receiver / preheater will be 0.017UL. Supposing, also as first guess, the acceptance angle as 21^o, we can calculate that the equivalent area of the entrance in 1+6 CPCs is $0.955UL^2$, corresponding at a diameter of 0.11UL. The optimized field of heliostats has to reach the input into equivalent circle of 0.11UL (following named: *target*), (at least) 17MW at the design point (Equinox, Noon). Another

important requirement is that the annual energy collected in this target must be at least 50GWh. Mentioned that the direct normal insolation is given for one day characteristic for each month, at each hour between 6AM and 7PM (matrix of 12x14 values). For the first guess, the vertex of hyperboloid is fixed at $\boldsymbol{fh}$=0.8UL.

As the first step, is calculated the power entered target at the design point, for various acceptance angles, and it is established the value of the CPC's acceptance angle which maximize this power.

The second step is to calculate the annual performances, i.e. the energy entered target along the year (for each hour between 6AM to 7PM, for each representative day per month, times the number of day in that month). The code calculates the energy collected due to each heliostat from the field represented in Fig.13.

In the third step, the heliostats are arranged decreasing, accordingly to their energetic contribution. Of course the sum of energy given from the entire field from the Fig.3 is much larger than the requirement (50GWh). Therefore the code performs a sum of energetic contribution of each heliostat until a limit of 50GWh. The layout of these heliostats is represented in Fig. 14. The heliostats included in this amount will mark the input field for the next step. In this field are included 2561 heliostats. The method of calculus used until now, is the ray tracing with a big initial number of rays. Increasing the number of rays used for trial, maybe the field can received a more smoothing boundaries, but the calculus is large time consuming and, for us, the fig. 14 give sufficient information to smooth the field and to arrive at the layout from the Fig.15.

The last step is to establish finally the CPC's dimensions based on annual performances that must be recalculated replacing the target circle with true heliostats. In order to cover all collector surfaces, the entrance in CPC is a hexagon as in Fig.16.

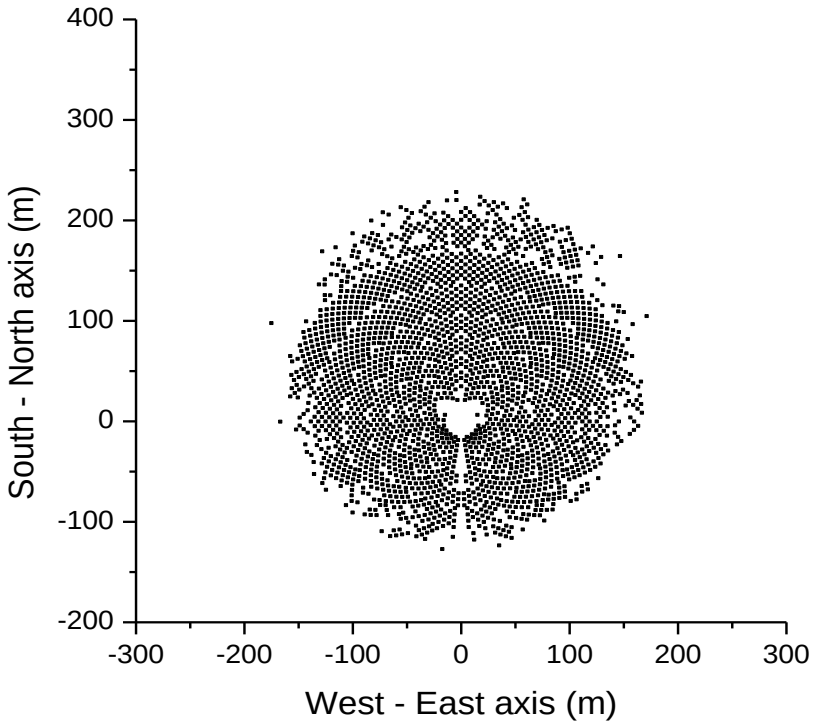

Fig. 14 Field resulted after classification of the best heliostats

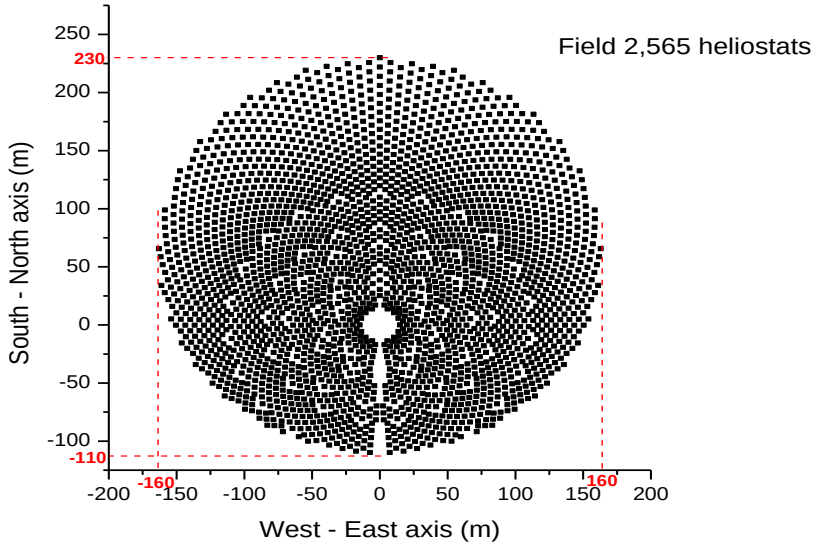

Fig. 15 Smoothed field based on field presented in Fig.14

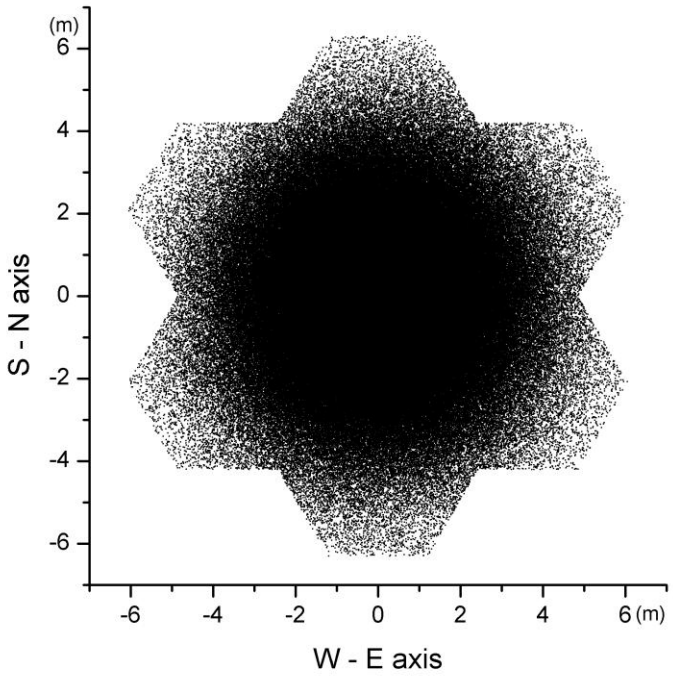

Fig. 16 Ray traces at the entrance plane in CPCs cluster

5. CONCLUSIONS

The present report describes in detail the mathematical principles which constitute the basis for Beam-Down Optics. In order to use this optics for central solar towers, few new requirements are imposed when an adequate heliostat layout has to be built. In the present, for this purpose, few codes working in a chain are used and the report presents the results that will be obtained in each step. Appropriate software that unified these codes in a single package is almost ready, but a user manual has to be written.

6. REFERENCES

Epstein M. and Segal A. (1998) A new concept for a molten salt receiver/storage system. In *Proceedings of Solar 98: Renewable Energy for Americas, Solar Engineering 1998, ASME International Solar Energy Conference,* 13–18 June, Albuquerque, NM, USA, Morehouse J. M. and Hogan R. E. (Eds), pp. 383–390.

Kistler, B.L. (1986) A user's manual for DELSOL3: A computer code for calculating the optical performance and optimal system design for solar thermal central receiver plants, Sandia National Laboratories, SAND86- 8018, Albuquerque, NM

Kribus A., Zaibel R., Carrey D., Segal A. and Karni J. (1997) A solar-driven combined cycle power plant. *Solar Energy* **62,** 121–129.

Kribus A., Zaibel R. and Segal A. (1998) Extension of the Hermite expansion for Cassegrainian solar central receiver systems. *Solar Energy* **63,** 337–343.

Lipps F.W. and Vant-Hull L.L,(978) A cellwise method for optimization of large central receiver systems, *Solar Energy*, **23**, 157-167.

Rabl A. (1976) Tower reflector for solar power plants. *Solar Energy* **18,** 269–271.

Ries H., Kribus A. and Karni J. (1995) Nonisothermal receivers. *Trans. ASME J. Solar Energy Eng.* **117,** 259–261.

Segal A. and Epstein M. (1996) A model for optimization of a heliostat field layout. In *Proceedings of 8th International Symposium on Solar Thermal Concentrating Technologies*, 6–11 Oct., Köln, Germany, Becker M. and Böhmer, M. (Eds), pp. 989–998. C.F. Müller Verlag, Heidelberg.

Segal A. and Epstein M. (1997) Modeling of solar receiver for cracking of liquid petroleum gas. *Trans. ASME J. Solar Energy Eng.* **119,** 48–51.

Segal A. and Epstein M. (1999a) Comparative performances of tower-top and tower-reflector central solar receivers. *Solar Energy* **65,** 206–226.

Segal A. and Epstein M. (1999b) The reflective solar tower as an option for high temperature central receivers. In *Proceedings of 9th SolarPACES International Symposium on Solar Thermal Concentrating Technologies*, 22–26 June 1998, Font-Romeu, France, *J. Phys. IV* **9,** Flamant G., Ferrière A. and Pharabod F. (Eds), pp. Pr3-53–Pr3-58.

Segal A. and Epstein M. (2000) Potential efficiencies of a solar-operated gas turbine and combined cycle, using the reflective tower optics. In *Proceedings of ISES Solar World Congress*, 4–9 July 1999, Jerusalem, Israel.

Segal A. and Epstein M.(2008) Practical consideration in designing large scale “Beam – Down” optical system, *ASME J.Solar Energy Eng.*, **139**, p.011009.

Winston R., Minano J.C., Benitez P. (2005), *Nonimaging Optics*, Elsevier Ac.Press, Amsterdam.

Winter C.-J., Sizmann R. L. and Vant-Hull L. L. (Eds) (1991*) Solar Power Plants: Fundamentals, Technology, Systems, Economics*. Springer-Verlag, Berlin.

Yogev A., Epstein M., Kogan A. and Kribus A. (1998) Solar tower reflector systems: A new approach for high-temperature solar plants. *Int. J. Hydrogen Energy* **23,** 367–376